Design of an Intent Recognition System for Dynamic, Rapid Motions in Unstructured Environments

Pooja R. Moolchandani
Georgia Institute of Technology
pmoolchandani3@gatech.edu

Anirban Mazumdar, PhD
Georgia Institute of Technology
anirban.mazumdar@me.gatech.edu

Aaron J. Young, PhD
Georgia Institute of Technology
aaron.young@me.gatech.edu

In this study, we developed an offline, hierarchical intent recognition system for inferring the timing and direction of motion intent of a human operator when operating in an unstructured environment. There has been an increasing demand for robot agents to assist in these dynamic, rapid motions that are constantly evolving and require quick, accurate estimation of a user's direction of travel. An experiment was conducted in a motion capture space with six subjects performing threat-evasion in 8 directions, and their mechanical and neuromuscular signals were recorded for use in our intent recognition system (XGBoost). Investigated against current, analytical methods, our system demonstrated superior performance with quicker direction of travel estimation occurring 140 ms earlier in the movement and a 11.6° reduction of error. The results showed that we could even predict movement start 100 ms prior to the actual, thus allowing any physical systems to start up. Our direction estimation had an optimal performance of 8.8°, or 2.4% of the 360° range of travel, using 3-axis kinetic data. The performance of other sensors and their combinations indicate that there are additional possibilities to obtain low estimation error. These findings are promising as they can be used to inform the design of a wearable robot aimed at assisting users in dynamic motions, while in environments with oncoming threats.

1 Introduction

1.1 Overview

Unstructured environments, such as construction sites, search-and-rescue, and war-zone areas, are dynamic and uncertain. Performing tasks in such situations can be dangerous for a human operator, and thus there is a significant need for smart robotics to enhance human safety and task completion efficiency, leading to a recent push for robot agents to collaborate in human-robot teaming as wearable robots, humanoids, unmanned ground vehicles, and swarm robots [1–3]. When environments or tasks become more dynamic, wearable robots offer particular promise because they can leverage the superior agility and mobility of their human operators to provide physical assistance to augment human safety. Existing works in the field of wearable robots have heavily focused on using different controllers to provide assistance for steady state locomotion [2, 3]. While analytical methods and control theory have dominated the field, intent recognition can provide more accurate estimation of when and how to apply better assistance for augmenting the performance of human operators. More recently, intent recognition has been introduced to the field to estimate the needed assistance in repeated locomotion, such as walking or running, or specific scenarios, such as lifting or pathology-specific ambulation [4, 5]. Given the adaptability of intent recognition, we can utilize such machine learning techniques to solve many of the challenges posed by dynamic, nonlinear motions performed by human operators.

We are centering the interaction between the human operator and wearable robot on human behavior during dynamic motions. The novelty of this work is determining human intent of dynamic motions to improve reaction and task execution for wearable robots to smartly assist operators. If a robot misunderstands intention, it may impose forces that are counterproductive or even dangerous. We aim to rapidly classify timing and directions of travel of the human agent using intent recognition and determine which on-board sensors are most critical. The main contribution of this work is the design of an intent recognition system that can (1) hierarchically predict when a human intends to move and estimate the intended direction of movement, (2) reduce the error of direction classification compared to analytical methods for fast, accurate estimation of directions of travel, and (3) quantify the contribution of candidate sensors for this motion.

In this study, analytical methods (referred to as the baseline) have been used to determine directions of travel using temporal information, such as integrating inertial data. We hypothesize that intent recognition machine learning al-

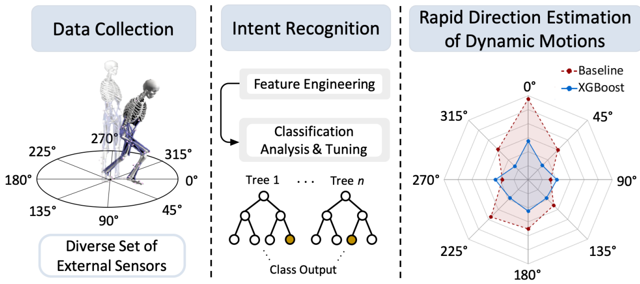

Fig. 1. Mechanical and physiological behavior captured through a human dynamic motion collection provides an intent recognition system the ability to optimize and estimate future motions

gorithms will reduce estimation error rate when classifying direction of movements compared to the baseline. In addition, another novel aspect of our approach is predicting future desire to initiate movement, a capability not possible using a purely analytical method. This work utilizes the following sensors to investigate performance: electromyography (EMG), inertial measurement units (IMUs), force plates, and motion capture markers. The system overview, shown in Fig. 1, relies on a multi-sensor collection of a human agent performing dynamic, nonlinear motions to predict the timing of movement start and estimate their direction of travel with our machine learning techniques.

1.2 Background

Control systems and analytical approaches have been used to track key metrics, such as position and orientation of robot agents [6–8]. Recent work has shown great promise with kinetic and inertial derivations [9, 10]. However, such methods may not be fast or accurate enough to predict and estimate dynamic behaviors that evolve as the movement progresses. In this study, we investigate the performance of such a baseline compared to our intent recognition system.

Intent recognition systems based in machine learning have been successful in the field of robotics for pattern recognition, socially assistive robots, and human-robot interaction [11, 12]. As a relatively recent development, machine learning for human movement and locomotion is seen in systems that provide assistance for various pathologies, prosthetic devices, and exoskeletons for walking using classification techniques [5, 13, 14]. As these studies get more specific to a certain type of use, there is a gap in the human motion intent field to design similar systems for more rapid, dynamic motions of the lower limbs [15–17]. Because intent recognition can enable rapid direction tracking of transient responses in other applications, we are examining sudden movements based in human motion intent since this rapid locomotion has not been explored yet with such techniques [18, 19].

The design of intent recognition systems for dynamic motions requires an initial prediction of when the movement is going to start during a human agent's reaction time followed by an immediate estimate of the direction of travel. Mechanical and physiological inputs can be used concurrently to capture the unique attributes of this motion and enhance estimating the intended direction of travel based off of previous work in classifying modes in locomotion [15, 16, 20]. Studies have investigated physiological methods on the lower limbs to understand the various components of movement [21–23]. Contact methods of monitoring muscle activation aid in measuring a quick response that is necessary for determining human motion intention and can serve as inputs into intent recognition systems [24, 25]. Moreover, they can start an intent recognition system during a predictive range, which is between the start of the human agent's reaction time and actual start of movement [19].

From the mechanical perspective, previous studies examine lower limb dynamics, such as inverse kinematics and inverse kinetics, to reveal information about the components and orientation of specific motions [26,27]. In human motion analysis, ground reaction forces (GRF), center of mass velocity, and center of pressure (CoP) have been key in analyses of various cases; therefore, their inclusion would provide important information for the intent recognition system [28,29]. Center of mass velocity has been a primary metric studied for gait tracking and was utilized in this work to determine when movement starts with precise and reliable motion capture [30]. Inertial sensors have also illustrated stable position tracking in unstructured environments [31, 32].

We developed a hierarchical architecture using mechanical and physiological sensors to predict movement start and estimate which direction an agent intended to move in order to provide rapid, optimized assistance for dynamic motions in unstructured environments. We obtained the overall system performance, which was defined as how fast and accurately we could estimate direction compared to an inertial baseline.

2 Methods

2.1 Experiment Procedure

A set of experiments was conducted to understand how subjects perform dynamic motions by collecting outputs from a set of external sensors during such movements. This study focused on direction-dependent motions. Six able-bodied subjects gave written, informed consent for a protocol that was approved by the Georgia Institute of Technology's Institutional Review Board (H18363).

Each subject stood in the middle of a six force plate configuration, which represented the center of a labeled circle (r = 2 m). Fig. 2 demonstrates the procedure of the experiment. 8 directions were chosen at 45° increments. After the subject was standing at rest for a randomized time (1 s – 10 s), a visual instruction of a top-down arrow of one of the 8 directions was displayed on a television. The subject was told to escape the labeled circle in the given direction as fast as they possibly could. This labeled circle ensured jumping and hopping were not performed since they were not representative of the more distinct, multiple step threat-evasion strategy. After successfully crossing the circle, the trial ended and the subject returned to their centered position. Each subject had a training period to become accustomed with the environment. The 8 directions and a null condition were tested

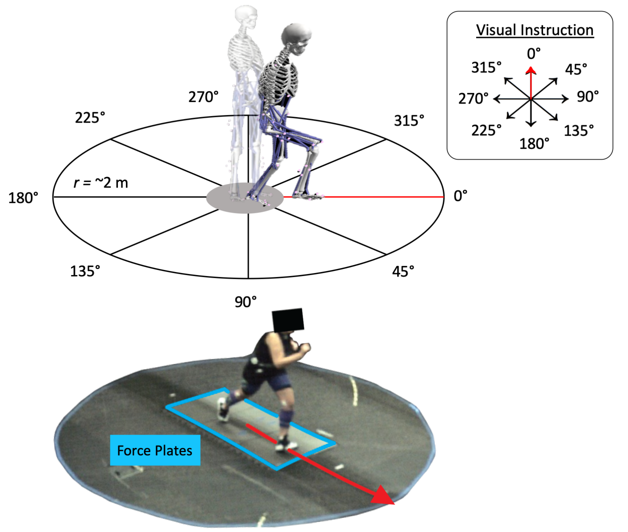

Fig. 2. Subjects, starting from rest, rapidly escaped a pre-labeled circle in the direction randomly displayed on a television. A subject is completing a trial in the 0° direction.

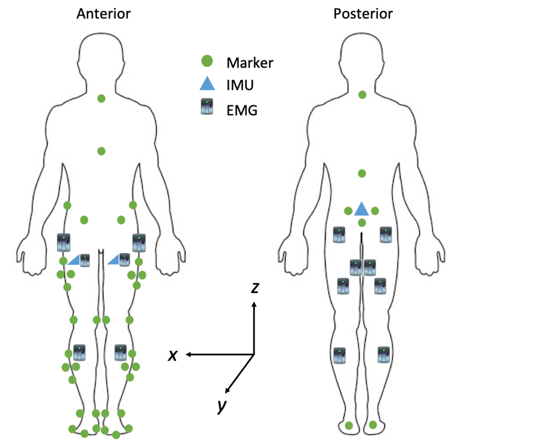

Fig. 3. Sensor and marker locations are annotated on anterior and posterior sides. EMG locations per lower limb were Tibialis Anterior, Rectus Femoris, Gastrocnemius Lateralis, Biceps Femoris, Tensor Fasciae Latae, Adductor Magnus, Gluteus Maximus. IMU locations were the Lower Back and the Left and Right Upper Thighs.

10 times, resulting in 90 trials per subject. The order of directions tested were randomized to prevent directional bias.

GRF and CoP were captured with six force plates (Bertec, Columbus, OH, USA). Three IMUs and 14 channels of EMG were placed on each subject (Delsys Avanti & Trigno Platforms, Natick, MA, USA). A 43-reflective marker set, modified from the Cleveland Clinic Standard Lower Limb Set, was also used in the motion capture space (Vicon, Oxford, UK). Sensor placements were illustrated in Fig. 3 [33].

2.2 Signal Processing

The collected sensor data shown in Fig. 3 was filtered as follows:

EMG: Muscle Activation, Bandpass (20-400 Hz)
IMU: 3-Axis Accelerometer (Accel), No Applied Filter
IMU: 3-Axis Gyroscope (Gyro), No Applied Filter
Force Plates: GRF, Lowpass (20 Hz)
Force Plates: CoP, Lowpass (20 Hz)
Motion Capture: Marker Trajectories, Lowpass (6 Hz)

In this study, EMG, IMU, GRF, and CoP were either already relative or transformed to the local body frame to be consistent with readings from most wearable sensors [34]. OpenSim v4.1 was used to calculate the sagittal and frontal hip joint angles [35]. GRFs were integrated to obtain impulse over time. For this dataset, we examined each trial for all directions from one second prior to the start of movement to before a limb made contact with ground outside of the force plate configuration.

To determine the key sensor information required for dynamic motions, the experiment data was grouped into three categories based on data retrievable from current sensors commonly used in wearable devices. These sensor groups are as follows:

1. *All Kinetic*: Vertical Kinetic + Shear Kinetic
   (a) *Vertical Kinetic*: Vertical GRF (1-axis) + CoP
   (b) *Shear Kinetic*: Horizontal GRF (2-axis) + Impulse
2. *EMG*: Muscle Activation
3. *Kinematic*: IMU (Gyro, Accel) + Hip Joint Angles

2.3 Intent Recognition Pipeline

An intent recognition pipeline using machine learning was created to predict and estimate threat-evasive behavior. Common practices in machine learning were utilized [5].

Supervised Learning: Type of model that trains on known inputs, or features, and known outputs, or labels. Performance is found by testing the model on known inputs but unknown outputs.
Binary Classification: Model that has only two possible outputs.
Multi-Class Classification: Model that has a known number of possible outputs >2.
Feature Engineering: Extraction technique to determine interesting attributes from a window of data to yield a set of representative values, or features, of that window.
Dimensionality Reduction: Reduction of dimensions in the feature space by selecting the optimal features that provide the most information.
Forward Feature Selection: Type of dimensionality reduction that iteratively adds features to the model to determine which set of features best improve the model's performance [36].
Sweep & Tuning: Optimization technique to find the best model parameters and hyperparameters through an exhaustive grid search.
Cross Validation: Evaluation method to determine a model's overall robustness by rotating out different testing sets.

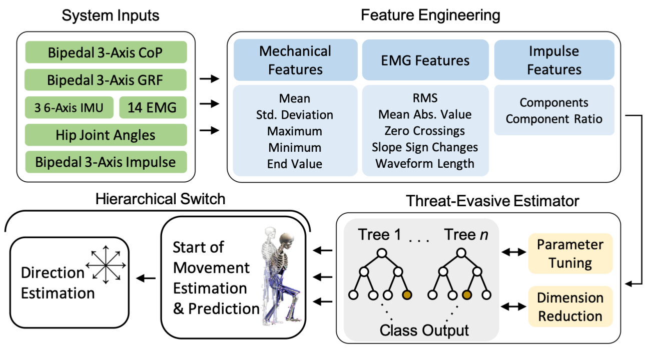

Fig. 4. Intent recognition pipeline illustrates the steps required from system inputs to feature engineering to optimization of algorithms in order to predict movement start and estimate direction of travel

Using the experiment outputs as system inputs after signal processing, as illustrated in Fig. 4, the inputs went through their respective feature engineering techniques [37]. The system was optimized with dimensionality reduction, a sweep of window sizes and increment lengths, and hyperparameter tuning before leading into the hierarchical structure to classify movement start and direction of travel.

The system was broken down into two models: 1) a timing model to predict when movement started from a resting position at the millisecond level, and 2) a direction model to estimate in what direction the subject intended to move. A selection of a machine learning algorithm for each of these models was needed. A case study of machine learning in human motion intent recognition has demonstrated that XGBoost, a new and robust machine learning algorithm, had the best performance in steady and transitional states of movement against current state-of-the-art models in the field [38]. XGBoost is a parallel tree boosting system that uses ensemble learning and gradient boosting to efficiently develop a set of trees from a supervised learning approach. Its benefits include regularization to prevent overfitting, controllable pruning of tree complexity, and working with sparse datasets [39]. It was selected for both timing and direction models.

2.3.1 Timing Model: Prediction & Sensor Optimization

The timing model used a form of supervised learning, binary classification (intended to move or not). Its ground truth label for start of movement, or the Absolute Kinematic Start, was based off of when the subject's center of mass velocity exceeded a set threshold compared to their resting position's velocity, using motion capture marker trajectories. Feature extraction was completed on the system inputs, excluding impulse. This omission was necessary as GRFs readings were not changing at rest, so impulse was negligible. The primary metric used for performance analysis was total classification error during the entire motion and classification error only during the transition window between no movement and movement.

Because the highest classification error in the binary timing model was likely to occur in this transition window, the timing model went through a prediction analysis in the transition phase, where Absolute Kinematic Start labels were changed to switch earlier than the actual start of movement. The estimation, *0 ms Prior*, was compared to predictions, *60 ms*, *100 ms*, *200 ms*, and *300 ms Prior* to Absolute Kinematic Start. These times were chosen to illustrate the progressive trend of predictions. Increment size for the model was 20 ms; therefore, selected predictive times were multiples of this increment. Forward feature selection was run at the best predictive time to determine the critical features that obtain low error. The sensor groups were analyzed at the best predictive time by their classification errors during the transition window. A one-way ANOVA was performed to determine statistical differences between the sensor groups with additional one-way ANOVA tests to compare different groupings.

2.3.2 Direction Model: Dimensionality Reduction, Estimation Over Time, & Estimation Per Direction

Once the Absolute Kinematic Start was reached, the direction model was activated. This model was formulated as a supervised, multi-class classification trained on the features in Fig. 4 and assigned labels as the displayed arrow on the television representing the intended direction of movement. Each direction represented a class. The primary performance metric for this model was mean absolute error (MAE) for a directional analysis of degrees.

Forward feature selection was executed to determine the optimal number of features for best performance and its contributing sensors. The results of the direction model were cross validated ($k = 2$) during dimensionality reduction and hyperparameter optimization. The hyperparameters tuned were the learning rate, maximum allowable tree depth, and minimum gain to split a tree node.

The performance of the direction model was evaluated with all directions compounded by the average estimation errors of various sensor groups and their combinations. A one-way ANOVA with a Bonferroni correction ($\alpha = 0.05$) for pairwise comparison was conducted to distinguish which group of sensors significantly reduced estimation error. Error over time was also analyzed to determine which sensor suite could provide a precise, continued estimation as the dynamic motion evolved. Directions were then examined separately, and the optimal error for each direction was reported at when 95% of the stabilized estimation error was reached in time.

2.3.3 Kinetic Baseline: Direction Estimation Over Time & Performance Per Direction

After developing and optimizing the timing and direction models of the intent recognition system, the next step was to compare our architecture against the direction estimation of an analytical approach common in similar works. After a preliminary testing of analytical methods found with wearable sensors (data not shown), we chose the best performing method, which was to calculate the total impulse from GRFs. The baseline was established as a kinetic response because of its advantageous performance, both spatially and temporally, unlike other sensors [40]. Therefore, the comparison of the kinetic baseline against the intent

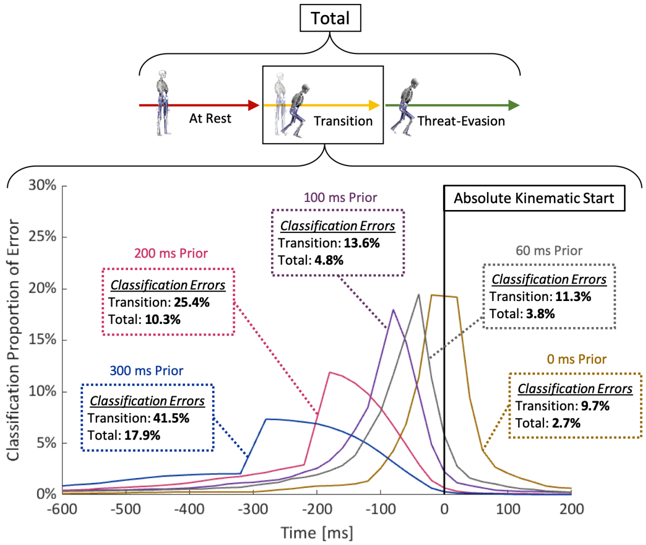

Fig. 5. The transition phase was examined for estimation (*0 ms Prior*) and predictions (*60 ms Prior, 100 ms Prior, 200 ms Prior, 300 ms Prior*) of the start of threat-evasive movement, or Absolute Kinematic Start. Steady state error for the estimation system was extremely low ($< 3\%$); thus, the primary differentiator was error during the specified transition window. Data zoomed to transition window.

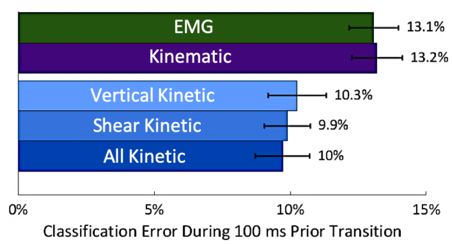

Fig. 6. The timing model's classification performance was examined by sensor groups at *100 ms Prior* to Absolute Kinematic Start. Classification errors were averaged over six subjects and error bars represented +/-1 SEM.

recognition system was not biased in favor to the proposed system by using poor performing baselines. The direction of travel was determined from the impulse components as $\theta = atan2(impulse_y, impulse_x)$.

The XGBoost direction model was studied against the kinetic baseline to determine which method efficiently achieved low error of direction estimation over time and for each direction. For each direction examined separately, 8 paired t-tests evaluated the statistical differences in MAE for each direction between the XGBoost model and baseline. The reported error for the baseline was captured at the time of when the XGBoost model had reached 95% of its stabilized response to represent a precise comparison in time. Analysis was broken down further by cardinal (0°, 90°, 180°, 270°) and diagonal directions (45°, 135°, 225°, 315°).

3 Results

3.1 Timing Model: Prediction & Sensor Optimization

The timing model's performance in the transition phase in Fig. 5 showed an increasing classification error as predictions were pushed further back before Absolute Kinematic Start. As further predictive times were examined, there was an increasing spread in time in which the errors occurred over time and a linear increase in the total classification error of the entire motion. Classification during the transition window also worsened as more times prior were examined. At *300 ms Prior*, the transition classification error constituted the majority of total classification error.

The timing model's forward feature selection at *100 ms Prior* indicated that the critical features to obtain a total error of 4.8% were vertical GRFs (left and right limbs) and IMU Gyro (left limb). The sensor group breakdown of the timing model in Fig. 6, which was trained at *100 ms Prior*, illustrated statistical differences in all five standalone sensor groups ($p < 0.05$). Additional one-way ANOVA tests demonstrated that All Kinetic, Kinematic, and EMG as well as Shear Kinetic, Kinematic, and EMG had statistical differences, meaning these kinetic groups performed better in error reduction than the EMG and Kinematic sensor groups ($p < 0.05$). However, Vertical Kinetic, EMG, and Kinematic ($p = 0.08$) as well as only the three kinetic groups ($p = 0.93$) demonstrated no statistical difference in error reduction. These findings indicate a statistically superior performance of the Shear Kinetic sensor group both standalone and in combination with the Vertical Kinetic sensor group.

3.2 Direction Model: Dimensionality Reduction

The direction model's forward feature selection demonstrated that the estimation error quickly decreased as features were individually added to the model, illustrated in Fig. 7. The optimal feature set was found when the added features no longer had any significant reduction in error, which corresponded to 13.8° MAE. The optimal features were segmented by sensor group to demonstrate the trend of the large contribution of kinetic data. From the set of features that produced the optimal error listed in Fig. 8, shear components of the kinetic data were common earlier in the set, meaning they greatly assisted in the error reduction. Additionally, out of the 7 muscles per limb examined, only 4 of the muscles were selected in this set: Bicep Femoris, Adductor Magnus, Tibialis Anterior, and Gastrocnemius Lateralis. The kinematic contribution in this optimized set included all 3 IMUs.

3.3 Direction Model: Estimation Breakdown & Performance Over Time

As combinations of the sensor groups in Fig. 9 were examined with the post-hoc pairwise comparison, EMG, Kinematic, and Vertical Kinetic groups had worse average degree errors than the kinetic baseline. The grouping of two or more sensors as well as the shear sensors alone produced a lower error than the baseline. The Vertical Kinetic group showed significant improvement in its estimation error as either Kinematic or Shear Kinetic groups were added to form

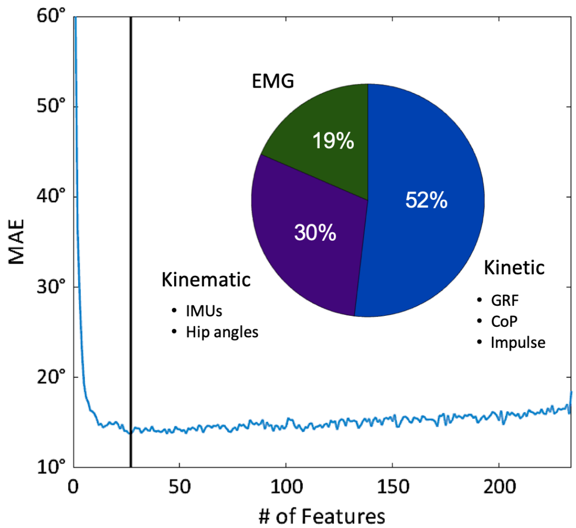

Fig. 7. Forward feature selection of the direction model was performed, and an optimal error was found at n = 27 features. The breakdown of this feature set is also illustrated.

Input	Feature	Input	Feature
1. Shear GRF *(y, r)*	Minimum	15. Hip Frontal Angle *(l)*	Standard Deviation
2. Shear Impulse *(x)*	-	16. IMU Gyro *(x, l)*	Mean
3. Shear CoP *(y, r)*	Maximum	17. IMU Gyro *(x, r)*	End Value
4. Shear Impulse *(y)*	-	18. EMG: Tibialis Anterior	Slope Sign Change
5. EMG: Bicep Femoris	RMS	19. IMU Gyro *(y, l)*	Mean
6. Shear CoP *(y, l)*	Maximum	20. IMU Gyro *(z, c)*	Mean
7. Shear GRF *(x, r)*	Mean	21. IMU Gyro *(x, r)*	Standard Deviation
8. Shear GRF *(x, l)*	Minimum	22. Shear CoP *(y, r)*	Mean
9. IMU Gyro *(y, c)*	Standard Deviation	23. Shear GRF *(y, l)*	End Value
10. EMG: Adductor Magnus	Wavelength	24. EMG: Adductor Magnus	Mean Absolute Value
11. Shear CoP *(y, r)*	End Value	25. Shear CoP *(y, l)*	Minimum
12. Vertical GRF *(z, r)*	Minimum	26. EMG: Gastrocnemius Lateralis	Zero Crossings
13. CoP *(x, l)*	End Value	27. IMU Gyro *(y, c)*	End Value
14. Shear GRF *(x, r)*	Minimum		

l = Left Limb *r* = Right Limb *c* = Center of Mass of Body

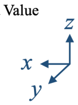

Fig. 8. The optimal set of features was determined using forward feature selection for the direction model

groups of two (Vertical Kinetic + Kinematic: $p = 0.02$, All Kinetic: $p < 0.0001$), but not when added with EMG (Vertical Kinetic + EMG: $p = 1.0$). As groups of three were examined against these groups of two, there was no significant improvement in any of these additions ($p > 0.05$), except when Shear Kinetic was included with Vertical Kinetic and EMG (All Kinetic + EMG: $p = 0.002$).

The addition of Shear Kinetic to any sensor group to form a group of two had significant reduction in error ($p < 0.05$ for all combinations of two). However, after Shear Kinetic was included to form a group of two, the addition of any other sensors to form a group of three or four had no statistically significant improvement in estimation error based on pairwise comparison. This indicated that Shear Kinetic sensors had optimal performance and greatly reduced estimation error as standalone and in combination with other sensor groups.

As subjects continued in their path, MAE over time was

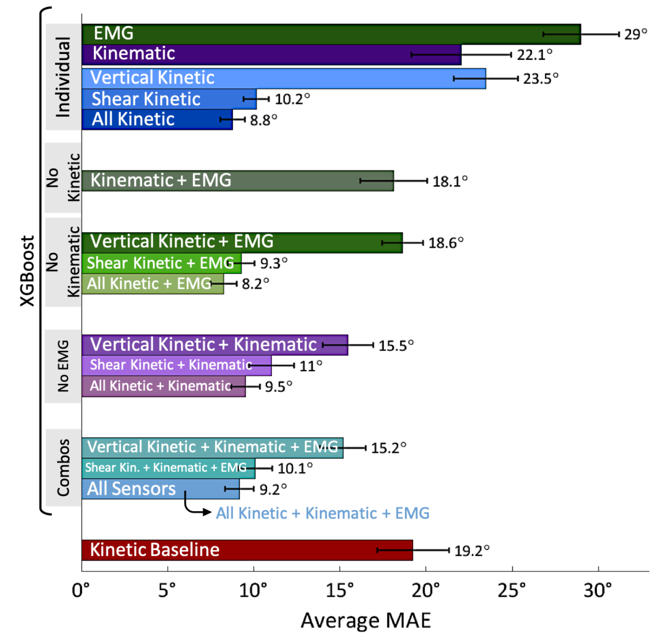

Fig. 9. For all directions compounded, the intent recognition system's direction model was trained by sensor group and their combinations. Average MAE was reported for each sensor group combination and the kinetic baseline. MAE was averaged over six subjects and error bars represent +/-1 SEM.

computed offline, as seen in Fig. 10, and demonstrated significantly better temporal performance of the direction model trained on the optimized feature set over the EMG sensor group, Kinematic sensor group, and kinetic baseline. The direction model trained on the All Kinetic sensor group had a similar performance to the model trained on the optimized feature set.

The kinetic baseline produced a stabilized response 500 ms into the evolution of the dynamic movement to MAE of 15.5°. The optimized feature set direction model had a stabilized response of 6.9° at 360 ms. The EMG direction model and Kinematic direction model stabilized later in the motion with both obtaining a minimization of error within the first 300 ms of movement. This minimum of MAE was consistent at the second toe-off of the stance leg.

3.4 Baseline vs. Direction Model Per Direction

At 95% of the intent recognition system's stabilized error shown in Fig. 11, the direction model consistently obtained error <15° for each direction, while the baseline varied between 5° and 45°. For three of the four cardinal directions, the intent recognition system had no significant improvement over the baseline (0°: $p = 0.024$, 90°: $p = 0.37$, 180°: $p = 0.05$, 270°: $p = 0.13$). However, the intent recognition system performed significantly better than the baseline in three out of the four diagonal directions (45°: $p = 0.01$, 135°: $p = 0.1$, 225°: $p = 0.003$, 315°: $p = 0.001$). This indicated that the intent recognition system was statistically better than the baseline in most diagonal directions and can match or outperform the baseline in all cardinal directions.

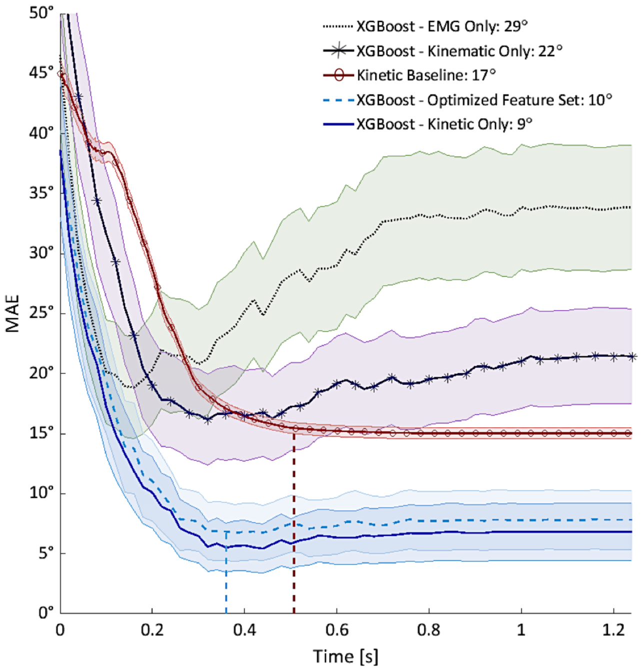

Fig. 10. The baseline's direction estimation was compared to the intent recognition system's estimation (XGBoost) over time by sensor group and optimized feature set. Annotated in the legend are these errors averaged across the time shown. The baseline had the greatest error than the other direction models' sensor breakdowns in the first 0.3 s of movement. Stabilized errors are shown as dotted lines for the respective analyses.

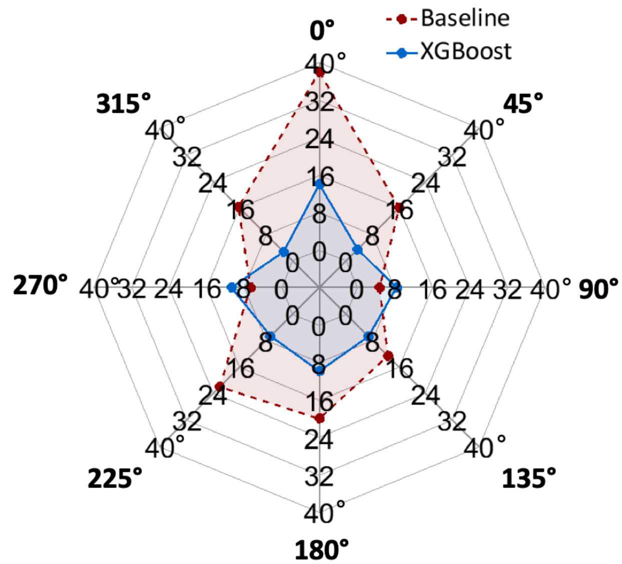

Fig. 11. For each direction analyzed, the intent recognition system's error at 95% of the steady state error was determined and averaged over six subjects. At the time of the intent recognition's annotated error, the baseline's error was found to illustrate the respective values according to an early estimation. The intent recognition's direction estimation (XGBoost) results presented used all available sensors.

4 Discussions

We successfully developed a hierarchical intent recognition system that 1) predicted movement start intent at *100 ms Prior* to Absolute Kinematic Start with a total classification error of 4.8% and 2) estimated movement direction within 8.8° of the correct vector with the optimal sensor suite of All Kinetic (Shear Kinetic and Vertical Kinetic). Additionally, the intent recognition system had significantly lower estimation error, consistent performance in all directions, and reached a steady state direction earlier than the baseline.

4.1 Predictive Timing for Intent Recognition System

The timing model's estimation of the Absolute Kinematic Start performed well due to low total classification error (<3%) and temporal performance with most of the error coming from the -50 ms to 50 ms range surrounding the switch between at rest and movement. Comparing this estimation to the predictive times, the percent increase of transition classification error for *60 ms Prior* was 17% and for *100 ms Prior* was 40%. The percent increase was 162% for *200 ms Prior* and 328% for *300 ms Prior*. Additionally, *200 ms Prior* and *300 ms Prior* had a larger spread in time where error occurred in this transition phase, while *60 ms Prior* and *100 ms Prior* did not. Therefore, as you look further before the start of movement, there is a disruption to the two surrounding phases, increasing the overall error of estimating the time of movement start. At *200 ms Prior* and *300 ms Prior*, the transition classification error constitutes a substantial portion of the total classification error, resulting in an inaccurate estimation of the switch. At *60 ms Prior*, the other phases are not as affected, and errors remain low. Under the same conditions, the findings at *100 ms Prior* are acceptable as well, and this predictive time looks further prior to Absolute Kinematic Start. These offline findings indicate that *100 ms Prior* is the optimal choice for a forward prediction window as it maintains low transition and total classification errors, while still predicting movement start without significantly affecting the other phases. Physical requirements of a wearable system can start up at this time, earlier than *0 ms Prior*. If the system is started too early at *200 ms Prior* or *300 ms Prior*, there would be a great loss in resolution. If the system is started at *60 ms Prior*, there is more time prior to the start of movement that the system can account for given the performance of *100 ms Prior*.

Compared to recent work on human motion estimation, our work provides a quicker, more general model with predictive capabilities. Other studies have examined different classification techniques for recognizing start of movement. In Lee's 2015 work, the motion classification of movement had good estimation for all but the deep learning approach [41]. Our XGBoost estimation method (<3% error) as well as our prediction capabilities (<5% error) perform better than their examined algorithms during movement estimation except the supervised MTRNN. However, XGBoost has lower computation time and is more flexible in its design. Additionally, it enhances our ability to predict earlier in time of when movement is about to occur rather than estimate, which is a new approach in the field. While some works rely heavily on EMG for predicting earlier times for dynamic motions, our findings indicate the All Kinetic sensor group is the optimal choice to monitor for movement start with better accuracy [19,42]. If needed, EMG and Kinematic sensors can be used to determine the predictive time for our problem, but with a 3% gain in error (Fig. 6). Now that Absolute Kinematic Start can be anticipated through this offline analysis, we can track dynamic motions over time as they are evolving with minimized delay to their actual movements.

4.2 Intent Recognition System's Direction Estimation & Sensor Contribution

Once the user has reached the Absolute Kinematic Start, we can proceed through the hierarchical architecture to user direction estimation. The intent recognition's direction estimation results provide the necessary temporal information, set of features, and sensor contributions to obtain the most advantageous sensor suite that produces a low error for accurate direction estimation of an agent. Kinetic sensors demonstrate a greater contribution in obtaining precise direction estimation than Kinematic and EMG sensors, as seen in its prevalence in the optimized feature set (Fig. 7), its role in greatly reducing error in its addition to sensor combinations (Fig. 9), and its significantly lower error over time (Fig. 10), averaged at 9°.

Our findings show that the inclusion of Shear Kinetic sensors drive the boost in performance of direction estimation. Shear Kinetic sensors can be combined with Vertical Kinetic sensors to produce the lowest, statistically-significant direction estimation error of 8.8°, which is a 2.4% error of the 360° range of potential directions. If Shear Kinetic sensors are readily available, EMG and Kinematic sensors would not be required for precise direction estimation; however, Shear Kinetic sensors are difficult to engineer, and very few wearable sensors and devices have them fully integrated to date. If these sensors are not accessible, our results indicate that combining sensor groups can reduce both averaged and temporal direction estimation error. Specifically, Vertical Kinetic and Kinematic sensor groups used together produce a direction estimation error of 15.5°, or a 4.3% error of the 360° range (Fig. 9). This combination has no statistical difference if EMG was included in this set.

Previous work has relied on kinematic data to provide orientation estimation. Aminian's work on lower limb orientation relied solely on inertial sensors and had a 1.7° error in thigh orientation estimation for fast movements in a 30° range of joint movement, which is 5.7% error [43]. Our work can obtain half that error with 3-axis kinetic data in a much wider range of movement.

An interesting minimization of error was found to correspond to a specific gait event during threat-evasion (Fig. 10). The minimization occurred earliest for the EMG sensor group as muscle activity foreshadows mechanical action. This trackable event of the second toe-off from the stance leg is a possible estimation technique for real-time implementation of this system. Previous literature demonstrates that online gait phase detection is possible with one or more sensors [16].

4.3 Performance Comparison of Baseline and Intent Recognition

The kinetic baseline method was compared to our algorithm architecture's direction estimation. The kinetic baseline took about 140 ms longer to reach a steady state response than the direction model with the optimized feature set (Fig. 10). Given the need for rapid, accurate estimation, the baseline method would not be sufficient to provide correct direction estimation for a user in a timely manner because it had greater error in the first 300 ms of threat-evasion and stabilized to a steady state error later and worse than the optimized XGBoost direction model. Our architecture provides fast, accurate estimations of agile motion much closer to their actual start of threat-evasion. Similar to our kinetic baseline, other works have focused on an analytical approach, such as orientation sensors, to estimate direction. There are drawbacks to using an analytical method to inform direction. One study showed increased difficulty at estimating negative angles and an error of 18.1° in the yaw angle [44]. As we fuse sensor groups together, we are making our estimation faster and more accurate.

The intent recognition system had a more uniform performance for each direction and was more versatile in its ability to estimate a variety of directions than the baseline. The baseline could be used for moving in the cardinal directions, but it had poorer performance than the intent recognition system for the diagonal directions. As such, other works have focused only on one plane of travel and inertial components since it has been shown as one of the best strategies in literature [10,45]. We have developed a method that is more robust than the kinetic approach and allows for a wider range of possible directions to be examined with precise direction estimation of dynamic motions.

4.4 Limitations

The error estimation and performance characterized in this study are reflective of noise and inaccuracies in the sensors used. We chose to include sensors that could be implemented in real-world applications in order to add to the robustness of translating this system to an online analysis. A few of the sensors were standard wearable sensors that could be embedded easily in wearable applications, such as EMG and IMUs. Other sensor readings were laboratory-grade, such as GRFs and some kinematic data, and would likely be less precise in a wearable application.

Although we have shown that 3D GRF (shear and vertical) sensors greatly improve the direction model's performance in this work, our offline analysis utilizes shear sensing with high-precision, 6-DOF force plates. Translating such measurements to a wearable system is not easy, but force sensing insoles may be a viable future option. Researchers continue to develop insoles capable of measuring 3D GRF and have shown MAEs of $< 10\%$ [46,47]. Sensor errors will reduce classification performance, and their metrics (noise and bias) will have to be rigorously analyzed either through perturbation analyses or new experiments.

5 Conclusions

This study contributed a design of an intent recognition system that quantified and determined candidate sensors best suited for dynamic, rapid motions as well as hierarchically predicted motion intent offline and reduced direction classification error once the estimation of direction of travel pipeline was activated. This work indicated that our intent recognition system would provide critical information in a precise and timely manner to interpret user intention when performing threat-evasive motions. These findings can inform the design of a wearable device to provide physical assistance for users dynamically evading oncoming threats in unstructured environments to protect human safety.

Acknowledgements

This research is supported in part by the National Science Foundation (NSF) National Robotics Initiative (NRI) 1830498, NSF Traineeship Program (NRT) 1545287.

References

[1] Goodrich, M. A., and Schultz, A. C., 2008. *Human-robot interaction: a survey*. Now Publishers Inc.

[2] Young, A. J., and Ferris, D. P., 2016. "State of the art and future directions for lower limb robotic exoskeletons". *IEEE Transactions on Neural Systems and Rehabilitation Engineering,* **25**(2), pp. 171–182.

[3] Hirai, K., Hirose, M., Haikawa, Y., and Takenaka, T., 1998. "The development of honda humanoid robot". In Proceedings. 1998 IEEE International Conference on Robotics and Automation (Cat. No. 98CH36146), Vol. 2, IEEE, pp. 1321–1326.

[4] Hofmann, A. G., and Williams, B. C., 2007. "Intent recognition for human-robot interaction.". In Interaction Challenges for Intelligent Assistants, pp. 60–61.

[5] Halilaj, E., Rajagopal, A., Fiterau, M., Hicks, J. L., Hastie, T. J., and Delp, S. L., 2018. "Machine learning in human movement biomechanics: best practices, common pitfalls, and new opportunities". *Journal of biomechanics,* **81**, pp. 1–11.

[6] Huo, W., Mohammed, S., Moreno, J. C., and Amirat, Y., 2014. "Lower limb wearable robots for assistance and rehabilitation: A state of the art". *IEEE systems Journal,* **10**(3), pp. 1068–1081.

[7] Kuo, C.-H., et al., 2016. "Trajectory and heading tracking of a mecanum wheeled robot using fuzzy logic control". In 2016 International Conference on Instrumentation, Control and Automation (ICA), IEEE, pp. 54–59.

[8] Erden, M. S., and Tomiyama, T., 2010. "Human-intent detection and physically interactive control of a robot without force sensors". *IEEE Transactions on Robotics,* **26**(2), pp. 370–382.

[9] Jung, S., Hsia, T. C., and Bonitz, R. G., 2004. "Force tracking impedance control of robot manipulators under unknown environment". *IEEE Transactions on Control Systems Technology,* **12**(3), pp. 474–483.

[10] Aguirre-Ollinger, G., Colgate, J. E., Peshkin, M. A., and Goswami, A., 2012. "Inertia compensation control of a one-degree-of-freedom exoskeleton for lower-limb assistance: Initial experiments". *IEEE Transactions on Neural Systems and Rehabilitation Engineering,* **20**(1), pp. 68–77.

[11] Croft, D., 2003. "Estimating intent for human-robot interaction". In IEEE international conference on advanced robotics, Citeseer, pp. 810–815.

[12] Yang, S. X., and Meng, M., 2000. "An efficient neural network approach to dynamic robot motion planning". *Neural networks,* **13**(2), pp. 143–148.

[13] Varol, H. A., Sup, F., and Goldfarb, M., 2009. "Multiclass real-time intent recognition of a powered lower limb prosthesis". *IEEE Transactions on Biomedical Engineering,* **57**(3), pp. 542–551.

[14] Begg, R., and Kamruzzaman, J., 2005. "A machine learning approach for automated recognition of movement patterns using basic, kinetic and kinematic gait data". *Journal of biomechanics,* **38**(3), pp. 401–408.

[15] Young, A. J., Simon, A. M., Fey, N. P., and Hargrove, L. J., 2014. "Intent recognition in a powered lower limb prosthesis using time history information". *Annals of biomedical engineering,* **42**(3), pp. 631–641.

[16] Huang, H., Zhang, F., Hargrove, L. J., Dou, Z., Rogers, D. R., and Englehart, K. B., 2011. "Continuous locomotion-mode identification for prosthetic legs based on neuromuscular–mechanical fusion". *IEEE Transactions on Biomedical Engineering,* **58**(10), pp. 2867–2875.

[17] Young, A., Kuiken, T., and Hargrove, L., 2014. "Analysis of using emg and mechanical sensors to enhance intent recognition in powered lower limb prostheses". *Journal of neural engineering,* **11**(5), p. 056021.

[18] Criminisi, A., Shotton, J., and Konukoglu, E., 2012. "Decision forests: A unified framework for classification, regression, density estimation, manifold learning and semi-supervised learning". *Foundations and Trends® in Computer Graphics and Vision,* **7**(2–3), pp. 81–227.

[19] Gregory, U., and Ren, L., 2019. "Intent prediction of multi-axial ankle motion using limited emg signals". *Frontiers in Bioengineering and Biotechnology,* **7**.

[20] Joshi, D., and Hahn, M. E., 2016. "Terrain and direction classification of locomotion transitions using neuromuscular and mechanical input". *Annals of biomedical engineering,* **44**(4), pp. 1275–1284.

[21] Irastorza-Landa, N., Sarasola-Sanz, A., López-Larraz, E., Bibián, C., Shiman, F., Birbaumer, N., and Ramos-Murguialday, A., 2017. "Design of continuous emg classification approaches towards the control of a robotic exoskeleton in reaching movements". In 2017 International Conference on Rehabilitation Robotics (ICORR), IEEE, pp. 128–133.

[22] Rand, M. K., and Ohtsuki, T., 2000. "Emg analysis of lower limb muscles in humans during quick change in running directions". *Gait & posture,* **12**(2), pp. 169–183.

[23] Artemiadis, P. K., and Kyriakopoulos, K. J., 2009.

"Emg-based position and force estimates in coupled human-robot systems: Towards emg-controlled exoskeletons". In Experimental Robotics, Springer, pp. 241–250.

[24] Young, A. J., Smith, L. H., Rouse, E. J., and Hargrove, L. J., 2012. "Classification of simultaneous movements using surface emg pattern recognition". *IEEE Transactions on Biomedical Engineering,* **60**(5), pp. 1250–1258.

[25] Accogli, A., Grazi, L., Crea, S., Panarese, A., Carpaneto, J., Vitiello, N., and Micera, S., 2017. "Emg-based detection of user's intentions for human-machine shared control of an assistive upper-limb exoskeleton". In *Wearable Robotics: Challenges and Trends*. Springer, pp. 181–185.

[26] Havens, K. L., and Sigward, S. M., 2015. "Joint and segmental mechanics differ between cutting maneuvers in skilled athletes". *Gait & posture,* **41**(1), pp. 33–38.

[27] Koopman, B., Grootenboer, H. J., and De Jongh, H. J., 1995. "An inverse dynamics model for the analysis, reconstruction and prediction of bipedal walking". *Journal of biomechanics,* **28**(11), pp. 1369–1376.

[28] Kawamori, N., Newton, R., and Nosaka, K., 2014. "Effects of weighted sled towing on ground reaction force during the acceleration phase of sprint running". *Journal of sports sciences,* **32**(12), pp. 1139–1145.

[29] James, C. R., Sizer, P. S., Starch, D. W., Lockhart, T. E., and Slauterbeck, J., 2004. "Gender differences among sagittal plane knee kinematic and ground reaction force characteristics during a rapid sprint and cut maneuver". *Research quarterly for exercise and sport,* **75**(1), pp. 31–38.

[30] Adamczyk, P. G., and Kuo, A. D., 2009. "Redirection of center-of-mass velocity during the step-to-step transition of human walking". *Journal of Experimental Biology,* **212**(16), pp. 2668–2678.

[31] Yeo, S. S., and Park, G. Y., 2020. "Accuracy verification of spatio-temporal and kinematic parameters for gait using inertial measurement unit system". *Sensors,* **20**(5), p. 1343.

[32] Fong, D. T.-P., and Chan, Y.-Y., 2010. "The use of wearable inertial motion sensors in human lower limb biomechanics studies: a systematic review". *Sensors,* **10**(12), pp. 11556–11565.

[33] Rainoldi, A., Melchiorri, G., and Caruso, I., 2004. "A method for positioning electrodes during surface emg recordings in lower limb muscles". *Journal of neuroscience methods,* **134**(1), pp. 37–43.

[34] Kim, S., and Nussbaum, M., 2014. "Evaluation of two approaches for aligning data obtained from a motion capture system and an in-shoe pressure measurement system". *Sensors,* **14**(9), pp. 16994–17007.

[35] Delp, S. L., Anderson, F. C., Arnold, A. S., Loan, P., Habib, A., John, C. T., Guendelman, E., and Thelen, D. G., 2007. "Opensim: open-source software to create and analyze dynamic simulations of movement". *IEEE transactions on biomedical engineering,* **54**(11), pp. 1940–1950.

[36] Jain, A., and Zongker, D., 1997. "Feature selection: Evaluation, application, and small sample performance". *IEEE transactions on pattern analysis and machine intelligence,* **19**(2), pp. 153–158.

[37] Phinyomark, A., Limsakul, C., and Phukpattaranont, P., 2009. "A novel feature extraction for robust emg pattern recognition". *arXiv preprint arXiv:0912.3973*.

[38] Bhakta, K., Camargo, J., Donovan, L., Herrin, K., and Young, A., 2020. "Machine learning model comparisons of user independent & dependent intent recognition systems for powered prostheses". *IEEE Robotics and Automation Letters,* **5**(4), pp. 5393–5400.

[39] Chen, T., and Guestrin, C., 2016. "Xgboost: A scalable tree boosting system". In Proceedings of the 22nd acm sigkdd international conference on knowledge discovery and data mining, pp. 785–794.

[40] Dos'Santos, T., Thomas, C., Comfort, P., and Jones, P. A., 2018. "The effect of angle and velocity on change of direction biomechanics: An angle-velocity trade-off". *Sports medicine,* **48**(10), pp. 2235–2253.

[41] Yu, Z., and Lee, M., 2015. "Human motion based intent recognition using a deep dynamic neural model". *Robotics and Autonomous Systems,* **71**, pp. 134–149.

[42] Bi, L., Guan, C., et al., 2019. "A review on emg-based motor intention prediction of continuous human upper limb motion for human-robot collaboration". *Biomedical Signal Processing and Control,* **51**, pp. 113–127.

[43] Dejnabadi, H., Jolles, B. M., Casanova, E., Fua, P., and Aminian, K., 2006. "Estimation and visualization of sagittal kinematics of lower limbs orientation using body-fixed sensors". *IEEE Transactions on Biomedical Engineering,* **53**(7), pp. 1385–1393.

[44] Harms, H., Amft, O., Winkler, R., Schumm, J., Kusserow, M., and Tröster, G., 2010. "Ethos: Miniature orientation sensor for wearable human motion analysis". In SENSORS, 2010 IEEE, IEEE, pp. 1037–1042.

[45] Pappas, I. P., Keller, T., Mangold, S., Popovic, M. R., Dietz, V., and Morari, M., 2004. "A reliable gyroscope-based gait-phase detection sensor embedded in a shoe insole". *IEEE sensors journal,* **4**(2), pp. 268–274.

[46] Rosquist, P. G., Collins, G., Merrell, A. J., Tuttle, N. J., Tracy, J. B., Bird, E. T., Seeley, M. K., Fullwood, D. T., Christensen, W. F., and Bowden, A. E., 2017. "Estimation of 3d ground reaction force using nanocomposite piezo-responsive foam sensors during walking". *Annals of biomedical engineering,* **45**(9), pp. 2122–2134.

[47] Lincoln, L. S., Bamberg, S. J. M., Parsons, E., Salisbury, C., and Wheeler, J., 2012. "An elastomeric insole for 3-axis ground reaction force measurement". In 2012 4th IEEE RAS & EMBS International Conference on Biomedical Robotics and Biomechatronics (BioRob), IEEE, pp. 1512–1517.